

Article

Novel Cellulose Triacetate (CTA)/Cellulose Diacetate (CDA) Blend Membranes Enhanced by Amine Functionalized ZIF-8 for CO₂ Separation

Ayesha Raza ^{1,2}, Susilo Japip ¹, Can Zeng Liang ¹, Sarah Farrukh ², Arshad Hussain ³ and Tai-Shung Chung ^{1,4,*}

¹ Department of Chemical and Biomolecular Engineering, National University of Singapore, Singapore 117585, Singapore; ayesha.raza@scme.nust.edu.pk (A.R.); a0096057@u.nus.edu (S.J.); chelian@nus.edu.sg (C.Z.L.)

² Department of Chemical and Materials Engineering, National University of Sciences and Technology, Islamabad 44000, Pakistan; Sarah.farrukh@scme.nust.edu.pk

³ Department of Chemical and Energy Engineering, Pak-Austria University, Haripur 22621, Pakistan; arshad.hussain@fcm3.paf-iast.edu.pk

⁴ Department of Chemical Engineering, National Taiwan University of Science and Technology, Taipei 1061, Taiwan

* Correspondence: chencts@mail.ntust.edu.tw or chencts@nus.edu.sg; Fax: +65-67791936

Abstract: Currently, cellulose acetate (CA) membranes dominate membrane-based CO₂ separation for natural gas purification due to their economical and green nature. However, their lower CO₂ permeability and ease of plasticization are the drawbacks. To overcome these weaknesses, we have developed high-performance mixed matrix membranes (MMMs) consisting of cellulose triacetate (CTA), cellulose diacetate (CDA), and amine functionalized zeolitic imidazolate frameworks (NH₂-ZIF-8) for CO₂ separation. The NH₂-ZIF-8 was chosen as a filler because (1) its pore size is between the kinetic diameters of CO₂ and CH₄ and (2) the NH₂ groups attached on the surface of NH₂-ZIF-8 have good affinity with CO₂ molecules. The incorporation of NH₂-ZIF-8 in the CTA/CDA blend matrix improved both the gas separation performance and plasticization resistance. The optimized membrane containing 15 wt.% of NH₂-ZIF-8 had a CO₂ permeability of 11.33 Barrer at 35 °C under the trans-membrane pressure of 5 bar. This is 2-fold higher than the pristine membrane, while showing a superior CO₂/CH₄ selectivity of 33. In addition, the former had 106% higher CO₂ plasticization resistance of up to about 21 bar and an impressive mixed gas CO₂/CH₄ selectivity of about 40. Therefore, the newly fabricated MMMs based on the CTA/CDA blend may have great potential for CO₂ separation in the natural gas industry.

Keywords: zeolitic imidazolate frameworks; polymer blend; mixed matrix membrane; plasticization resistance; CO₂ separation



Citation: Raza, A.; Japip, S.; Liang, C.Z.; Farrukh, S.; Hussain, A.; Chung, T.-S. Novel Cellulose Triacetate (CTA)/Cellulose Diacetate (CDA) Blend Membranes Enhanced by Amine Functionalized ZIF-8 for CO₂ Separation. *Polymers* **2021**, *13*, 2946. <https://doi.org/10.3390/polym13172946>

Academic Editors: Yu-Hsuan Chiao and Ranil Wickramasinghe

Received: 12 August 2021

Accepted: 27 August 2021

Published: 31 August 2021

Publisher's Note: MDPI stays neutral with regard to jurisdictional claims in published maps and institutional affiliations.



Copyright: © 2021 by the authors. Licensee MDPI, Basel, Switzerland. This article is an open access article distributed under the terms and conditions of the Creative Commons Attribution (CC BY) license (<https://creativecommons.org/licenses/by/4.0/>).

1. Introduction

Natural gas is an attractive and relatively green energy source as compared to coal, mainly because of its lower carbon footprint [1–3]. However, depending on the geological location, raw natural gas varies substantially in composition and may contain 50–90 mole % methane together with other undesirable components such as H₂O, CO₂, H₂S, N₂, C₂H₆, C₃H₈, and toluene. The presence of CO₂ and H₂S can cause pipeline corrosion and reduce the caloric value of the natural gas [1,4,5]. Therefore, the demand of high-purity natural gas is increasing by the energy producers to enhance its calorific and economic values [5]. To purify raw natural gas, membrane technology has emerged as an alternative process due to its environmental and economic benefits [1,5]. In particular, polymeric membranes have led to the commercialization of membrane-based gas separations for various applications including CO₂ separation from natural gas [6–8]. To make the membrane-based gas separation more competitive over conventional separation technologies such as amine

absorption and cryogenic distillation, membranes with a higher selectivity and permeability are required [9–13]. Nevertheless, the design of high-performance polymeric membranes is challenging mainly due to (1) the tradeoff relationship between permeability and selectivity of the polymeric materials [14] and (2) the plasticization phenomenon because the highly condensable gases like CO₂ tend to drastically reduce membrane selectivity [15–17].

Tremendous efforts have been made to overcome these constraints and to design novel membrane materials with high separation performance in terms of both gas selectivity and permeability [9–11,18]. Among these efforts, polymer blends and mixed matrix membranes (MMMs) are the popular approaches because they are simple and effective [19,20]. Particularly, MMMs, which incorporate inorganic particles in the continuous phase of the polymer matrix, have gained growing interests [9,20–22]. In MMMs, the polymeric matrix offers low cost and easy processability as the major benefits, while inorganic components exhibit high permeability, selectivity, and good thermal stability. MMMs possess impressive gas separation performance due to the combined benefits of both polymeric and inorganic materials. Inorganic particles incorporated in MMMs as the dispersed phase can be classified into two major categories: (1) non-porous/impermeable fillers such as silica and TiO₂ and (2) porous/permeable fillers such as carbon nanotubes, zeolites, and metal organic frameworks (MOFs) [20,22].

Currently, MOFs, especially zeolitic imidazolate frameworks (ZIFs), have been receiving significant attention as potential porous fillers used in MMMs owing to their molecular sieving properties, good stability, and compatibility with the polymer matrices [23]. One of the most extensively studied ZIFs is ZIF-8, which is constructed by a sodalite crystal structure. It possesses a pore cavity of 1.16 nm that is reachable through a small pore aperture of 0.34 nm [23]. Among various ZIFs, ZIF-8 has shown a remarkable CO₂ separation performance [21,24,25] mainly because the aperture size of ZIF-8 is between the kinetic diameters of CO₂ and CH₄ (0.33 nm and 0.38 nm, respectively), thus enhancing the CO₂ diffusivity and permeability [26]. Nevertheless, pore blockage, rigidification of the polymeric chains, and particles agglomeration are the major challenges during the fabrication of MMMs [9,27,28].

Aside from MMMs, polymer blends [19,29–34] are one of the practical methods to tackle the aforementioned tradeoff relationship existing in polymeric membranes. Not only can they combine the desirable properties of different materials into the new blend with targeted performance, but they also minimize the deficiencies of the individual components. Apart from their advantages, the major challenge of polymer blends is their miscibility at molecular level [19]. For example, Sanaeepur et al. studied the gas separation performance of CA/Pebax blend membranes [32]. The membrane blended with 8 wt.% Pebax showed 29% and 59% increases in CO₂ permeability and CO₂/N₂ selectivity, respectively. Recently, Akbarzadeh et al. fabricated green blend membranes of thiazole-based polyamine (PM-4) and CA for CO₂ separation [33]. Their optimal membrane displayed an impressive CO₂ permeability of up to 3000 Barrer with a CO₂/CH₄ selectivity of around 34 obtained at a feed pressure of 3 bar and 35 °C. Lin et al. studied the effects of membrane thickness and CA blend composition of submicron films [34]. They found that the 75/25 (*w/w*) cellulose triacetate (CTA)/cellulose diacetate (CDA) blend film with a thickness of 1 μm had a CO₂ permeability of 14 Barrer, which was not only about 100% higher than the same blend membrane with a thickness of 20 μm (i.e., 14 vs. 7.1 Barrer), but also about 250% higher than the pristine CDA membrane (i.e., 14 vs. 3.9 Barrer). Their findings inspired us to employ CTA/CDA blends as the matrix materials for the fabrication of MMMs for CO₂/CH₄ separation.

Therefore, the objectives of this work are to (1) synergistically combine the strengths of MMMs and polymer blends and (2) design a novel membrane material for CO₂ separation from natural gas. To our best knowledge, the noteworthy combination of CTA/CDA–amine functionalized ZIF-8 polymer blend MMMs has not yet been explored. This would be the first study on the fabrication of CTA/CDA–NH₂–ZIF-8 blend MMMs and investigation of their CO₂/CH₄ separation performance as a function of NH₂–ZIF-8 loading. CTA and CDA

blends were chosen as the matrix material because they have similar chemical structures, good separation performance, and a cheap and environmentally friendly nature. NH_2 -ZIF-8 was used as a filler because its pore size is between the kinetic diameters of the separating gases (CO_2 and CH_4). Moreover, the NH_2 group attached on the surface of ZIF-8 has good affinity with condensable gases like CO_2 . This study may provide useful insights to design next-generation CA membranes for the purification of natural gas.

2. Experiments and Methods

2.1. Materials

Cellulose triacetate (CTA) with a degree of substitution (DS) of 2.87 and cellulose diacetate (CDA) with a DS of 2.45 were provided by Eastman Chemical Company (Kingsport, TN, USA), while N-methyl-2-pyrrolidone (NMP, >99.5%) was bought from Merck (Darmstadt, Germany). Zinc nitrate ($\text{Zn}(\text{NO}_3)_2 \cdot 6\text{H}_2\text{O}$), 2-methylimidazole, and ammonium hydroxide (NH_4OH) were purchased from Science Centre, Pakistan (Islamabad, Pakistan). Gas cylinders of CO_2 (purity $\geq 99.95\%$) and CH_4 (purity $\geq 99.95\%$) were supplied by Air Liquide Singapore Pte. Ltd. Singapore The chemical structures of CTA and CDA are shown in Figure 1A,B.

2.2. ZIF-8 Synthesis

A solvo-chemical method was employed to synthesize ZIF-8 nanoparticles as reported by Pan et al. [35]. In this process, $\text{Zn}(\text{NO}_3)_2 \cdot 6\text{H}_2\text{O}$ (1.17 g) and 2-methylimidazole (22.70 g) were dissolved separately in deionized (DI) water. The prepared solutions were stirred for a few minutes prior to the mixing and were continuously stirred at room temperature for another 12 h. The resultant milky solution was centrifuged, followed by washing with DI water. Afterwards, the washed product was dried in an oven at 65°C overnight.

2.3. Amine Modification of ZIF-8

Amine functionalization of ZIF-8 nanoparticles was carried out following the method reported by Nordin et al. [36], with some modifications. Briefly, NH_4OH (28 mL) and H_2O (10 mL) were slowly added to ZIF-8 (1 g) under constant stirring, followed by overnight sonication at 80°C . The resulting mixture was centrifuged and washed multiple times with distilled water to remove any impurities before being dried in a vacuum oven at 70°C for 12 h. The chemical structures of ZIF-8 and NH_2 -ZIF-8 are presented in Figure 1C,D, respectively [37].

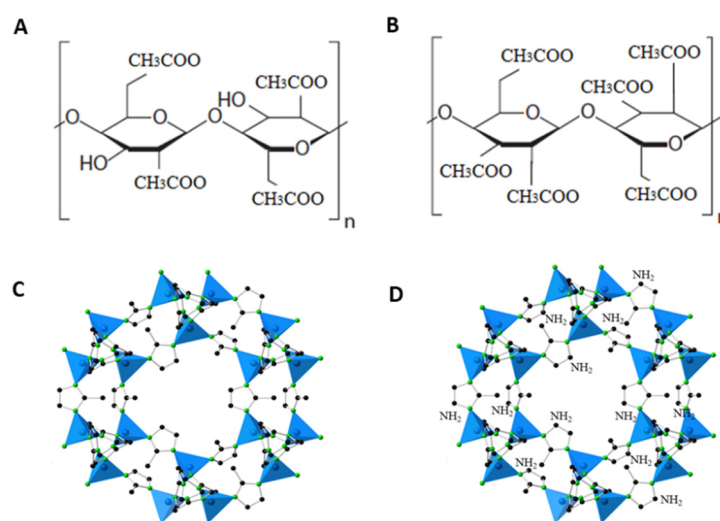


Figure 1. Chemical structure of (A) cellulose diacetate (CDA), (B) cellulose triacetate (CTA), (C) ZIF-8, and (D) NH_2 -ZIF-8, Reprinted with permission from ref. [37]. Copyright 2013 Springer Nature.

2.4. Membrane Fabrication

Solution casting and solvent evaporation techniques were used to fabricate dense membranes. CDA and CTA powders were dried in a vacuum oven at 120 °C overnight to remove moisture. The blend polymer consisting of 80/20 (wt.%) CTA/CDA was dissolved in NMP followed by vigorous stirring at 40 °C overnight until the solution became homogeneous. Separately, the NH₂-ZIF-8 and NMP suspension was sonicated for 2 h prior to mixing with the pre-prepared polymer blend solution. After mixing, the solution was stirred for 30 min and then cast on a clean glass plate by a casting blade, followed by solvent evaporation in a conventional oven at 100 °C overnight. The dried films were peeled off from the glass plate and dried in a vacuum oven at 120 °C for at least 24 h. The loading of NH₂-ZIF-8 was calculated using Equation (1) and varied from 0 to 15 wt.% based on the polymer weight. For example, a 5 wt.% NH₂-ZIF-8 MMM consists of 95 wt.% the blend polymer (i.e., 76 wt.% CTA and 19 wt.% CDA) and 5 wt.% NH₂-ZIF-8.

$$\text{Particle loading (\%)} = \frac{\text{weight of the particles}}{\text{weight of the particles} + \text{weight of the polymer}} \times 100 \quad (1)$$

2.5. Characterizations

The crystal structure of NH₂-ZIF-8 nanoparticles and the corresponding MMMs were analyzed by a Bruker wide-angle X-ray diffractometer (Bruker D8 advanced diffractometer, Bruker, Tokyo, Japan) using Cu-K α as a radiation source at a wavelength of 1.54 Å. The morphologies of the samples were examined by a field emission scanning electron microscope (FESEM, JEOL, JSM-6700LV, Tokyo, Japan). Prior to the inspection, the membranes were frozen and fractured in liquid nitrogen followed by platinum coating using a platinum (Pt) sputter coater (JEOL JFC-1300, Peabody, MA, USA). NH₂-ZIF-8 nanoparticles were directly glued on the surface of the sample holder before being coated. Chemical functionalities and interactions between polymers and nanofillers were confirmed by Fourier-transform infrared spectroscopy (FTIR, spectrum 100, Perkin Elmer, Beaconsfield, England, UK). The measurements were conducted between the wave numbers ranging from 4000 to 600 cm⁻¹. Thermal stabilities of pure NH₂-ZIF-8 nanoparticles and MMMs were examined by a Shimadzu Thermal Analyzer (DTG-60AH/TA-60WS/FC-60A, Shimadzu corporation, Tokyo, Japan). All samples were heated at a heating rate of 10 °C/min from room temperature to 800 °C under air atmosphere.

2.6. Gas Permeation Measurements

2.6.1. Pure Gas Tests

A constant volume variable pressure method was used to record the pure gas permeation properties. Detailed experimental setup and procedures can be found elsewhere [38]. All the membranes were tested at 35 °C under the trans-membrane pressure of 5 bar. For each membrane, at least three samples were tested and the average results were reported. The gas permeability was calculated based on the rate change of the downstream pressure increase (dp/dt) at steady state by using Equation (2)

$$P = \frac{273 \times 10^{10}}{760} \frac{VL}{AT(p_2 \times 76/14.7)} \frac{dp}{dt} \quad (2)$$

where P is the membrane permeability in Barrer (1 Barrer = 1×10^{-10} cm³(STP) cm/(cm² s cmHg), L is the membrane thickness (cm), V represents the volume of the downstream chamber (cm³), A is the effective membrane area (cm²), T signifies the operating temperature (K), and the upstream pressure is represented by p_2 (psia).

The ideal selectivity ($\alpha_{A/B}$) of two gases (A and B) was calculated according to Equation (3)

$$\alpha_{A/B} = P_A/P_B = (S_A/S_B) \times (D_A/D_B) \quad (3)$$

where P_A and P_B represent the permeability (Barrer) of gases A and B, respectively. S and D denote the solubility and diffusion coefficients of the gas, respectively. S_A/S_B and D_A/D_B are the solubility selectivity and diffusion selectivity of the gas pair, respectively.

The sorption behaviors of the blend membrane and the optimized MMM were evaluated using a XEMIS microbalance. Detailed experimental procedures can be found elsewhere [39]. Equation (4) was used to estimate the solubility coefficient (S , $\text{m}^3(\text{STP})/\text{cm}^3\text{cmHg}$) of the adsorbed gas inside the membrane at 5 bar, while the diffusivity coefficient (D , $10^{-8} \text{ cm}^2/\text{s}$) was calculated based upon Equation (5).

$$S = \frac{C}{p} \quad (4)$$

$$P = S \times D \quad (5)$$

where C represents the total adsorbed gas concentration ($\text{cm}^3(\text{STP})/\text{cm}^3$) and p is the feed pressure (cmHg).

2.6.2. Mixed Gas Tests

Mixed gas tests were carried out at 10 bar and 35 °C using a binary feed mixture of CO_2/CH_4 (50/50 v/v). The detailed experimental description can be found elsewhere [40]. The permeability for each gas was calculated using Equation (6)

$$P_i = \frac{273 \times 10^{10}}{760} \frac{y_i V L}{AT(76/14.7)(x_i p_2)} \frac{dp_1}{dt} \quad (6)$$

where P_i is the permeability of gas i , p_2 represents the upstream feed gas pressure (psia), p_1 is the downstream pressure (psia) of the permeate gas, x_i is the molar fraction of gas i in the feed gas stream and y_i is the molar fraction of gas i in the permeate, L is the membrane thickness (cm), and V signifies the volume of the downstream chamber (cm^3).

3. Results and Discussion

3.1. Characterizations

Figure 2 shows the weight loss profiles of the pure NH_2 -ZIF-8 nanoparticles, CTA/CDA blend membrane, and fabricated MMMs as a function of temperature. The NH_2 -ZIF-8 nanoparticles exhibited a gradual weight loss of around 9 wt.% from 30 to 450 °C owing to the removal of guest molecules trapped in the nanocrystals during synthesis and post treatment steps, followed by a steep decrease from 450 to 600 °C due to the framework decomposition. The findings are in good agreement with the reported thermal behavior of ZIF-8 [41,42]. The TGA thermogram of the pure CTA/CDA blend membrane revealed three weight-loss steps which are consistent with the literature [43–45]. The initial weight loss from 30 to 120 °C corresponded to the removal of volatile matters and moisture adsorbed by the membrane due to the hygroscopic nature of CA. The second major weight loss in the range of 310–400 °C symbolized the thermal degradation of the polymer followed by the third step due to the carbonization of degraded products to ash. Thermograms of MMMs also exhibited these three steps of weight loss and demonstrate good thermal stability up to 310 °C. Table 1 shows a significant improvement in decomposition temperature (Td) with an increase in NH_2 -ZIF-8 loading. The improvement in Td arose from (1) good compatibility and strong interaction between the filler and the polymer matrix and (2) inherent thermal characteristics of NH_2 -ZIF-8 nanoparticles. Thus, the incorporation of NH_2 -ZIF-8 into the CTA/CDA blend membrane hindered the chain movement and raised the energy requirement to decompose its polymer structure. A similar observation has been widely reported in the literature [46–48].

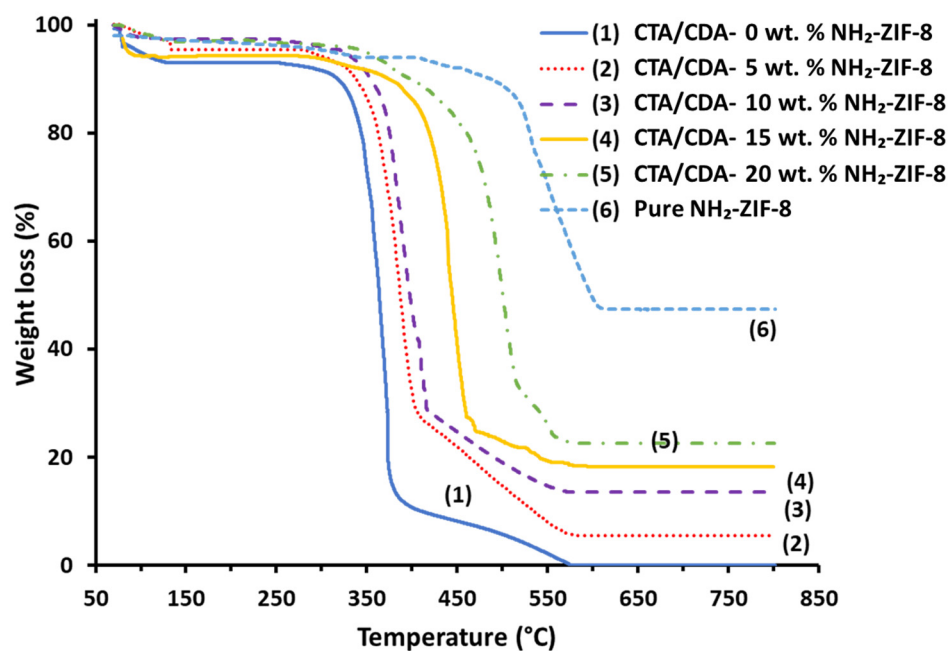


Figure 2. TGA of pure NH₂-ZIF-8 and CTA/CDA-NH₂-ZIF-8 MMMs with different NH₂-ZIF-8 loadings.

Table 1. Comparison of pure gas separation performance and decomposition temperature (Td) of CTA/CDA-NH₂-ZIF-8 MMMs with different NH₂-ZIF-8 loadings.

Sample Name	Actual NH ₂ -ZIF-8 Loading (%)	Td (°C)	Pure Gas Permeabilities (Barrer)		CO ₂ /CH ₄ Selectivity
			CO ₂	CH ₄	
CTA/CDA-0 wt.% NH ₂ -ZIF-8	0	310	7.56 ± 0.17	0.28 ± 0.02	27.00
CTA/CDA-5 wt.% NH ₂ -ZIF-8	5.13	320	8.10 ± 0.07	0.29 ± 0.03	27.93
CTA/CDA-10 wt.% NH ₂ -ZIF-8	10.58	338	9.52 ± 0.05	0.31 ± 0.01	30.71
CTA/CDA-15 wt.% NH ₂ -ZIF-8	15.80	363	11.33 ± 0.09	0.34 ± 0.02	33.32
CTA/CDA-20 wt.% NH ₂ -ZIF-8	22.37	390	13.20 ± 0.21	0.54 ± 0.01	24.44

Figure 3 displays the XRD patterns of the pure NH₂-ZIF-8 nanoparticles, CTA/CDA blend membrane, and their MMMs as a function of NH₂-ZIF-8 loading. The two main peaks at 2θ values of 8° and 17° confirm the semi-crystalline nature of the CTA/CDA blend membrane [49]. The XRD pattern of the NH₂-ZIF-8 nanocrystals was also in good agreement with the literature [50,51]. All the diffraction patterns of CTA/CDA-NH₂-ZIF-8 MMMs possessed the characteristic peaks of both NH₂-ZIF-8 and CTA/CDA moieties, signifying the preservation of their crystalline structures in the membranes. In addition, the intensity of the characteristic peaks of NH₂-ZIF-8 improved with an increase in its loading in MMMs.

FTIR spectra of NH₂-ZIF-8 nanoparticles and all fabricated membranes are compared in Figure 4. The CTA/CDA spectrum was characterized by major peaks at 3483, 2950, and 1750 cm⁻¹ corresponding to O-H, C-H, and C=O groups, respectively [52]. In contrast, the FTIR spectrum of NH₂-ZIF-8 nanoparticles was in good agreement with the reported literature [52,53]. The amine functionalization of ZIF-8 was also confirmed by the absorption peaks at ~1309 cm⁻¹ and 690 cm⁻¹ due to the NH₂ bonding on ZIF-8 molecules [54].

In summary, the FTIR spectra reconfirmed the existence of CTA/CDA and NH₂-ZIF-8 nanoparticles in all fabricated MMMs.

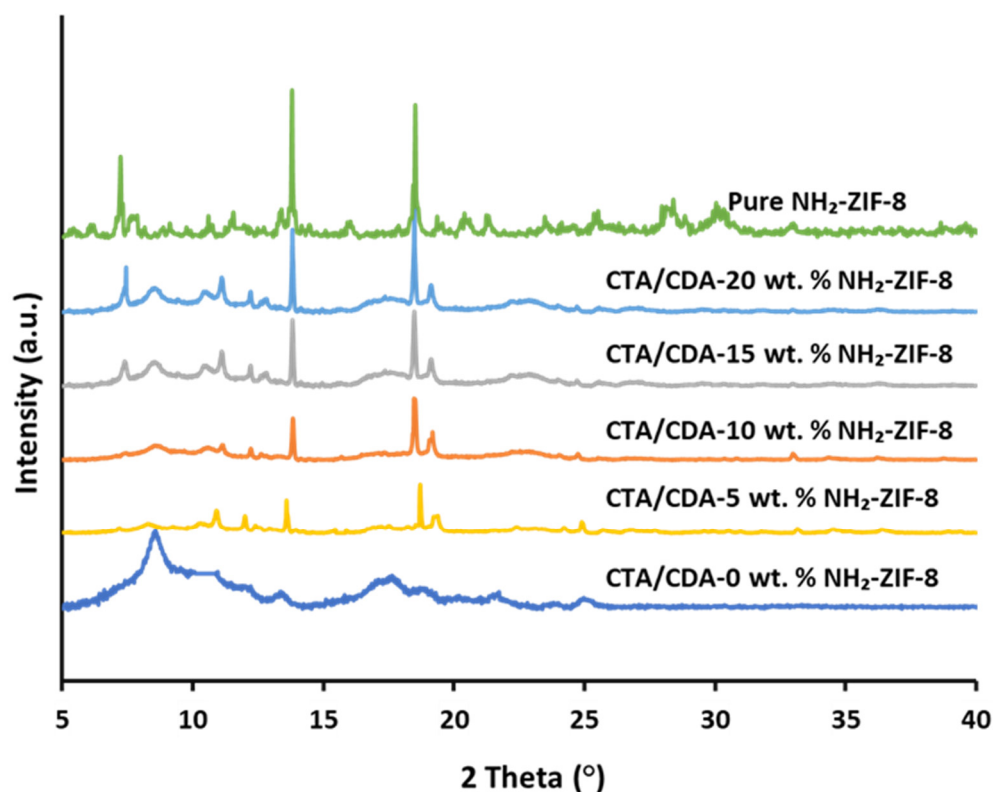


Figure 3. XRD analyses of pure NH₂-ZIF-8 and CTA/CDA-NH₂-ZIF-8 MMMs with different NH₂-ZIF-8 loadings.

Figure 5 displays the FESEM images of the pure NH₂-ZIF-8 nanoparticles, CTA/CDA blend membrane, and their MMMs as a function of NH₂-ZIF-8 loading. The NH₂-ZIF-8 nanoparticles had a size between 50 and 80 nm. Meanwhile, they were well dispersed in the CTA/CDA matrix with no clear evidence of interfacial gaps and phase separation. This signifies the good compatibility between the NH₂-ZIF-8 nanoparticles and CTA/CDA matrix because of (1) the small size of NH₂-ZIF-8 nanoparticles and (2) the formation of hydrogen bonds between the –NH₂ groups of NH₂-ZIF-8 nanoparticles and the –OH groups of the polymer matrix [5]. The uniform dispersion of NH₂-ZIF-8 nanoparticles was also confirmed by the energy-dispersive X-ray spectroscopy (EDX). Figure 6 shows the mapping of Zn particles in the MMMs with variable loadings. Since the polymer matrix did not contain any Zn element, the uniform dispersion of Zn element verified the uniform dispersion of NH₂-ZIF-8 nanocrystals in the polymer matrix.

3.2. Gas Transport Properties

Pure gas separation performances of the CTA/CDA blend membrane and CTA/CDA-NH₂-ZIF-8 MMMs are shown in Figure 7. Table 1 tabulates the detailed results. Both CO₂ and CH₄ permeabilities exhibited noticeable increases as a function of NH₂-ZIF-8 loading. However, the CO₂/CH₄ selectivity exhibited an up and down trend. A similar trend was observed for polyimide-ZIF-8 MMMs in the literature [55]. Generally, the incorporation of nanofillers in the polymer matrix disrupts the packing of polymeric chains, which may result in additional free volume and diffusion paths for gas transport [56]. Therefore, the CTA/CDA-15 wt.% NH₂-ZIF-8 membrane had a 50% increase in CO₂ permeability from 7.56 to 11.33 Barrer and a 23% increase in CO₂/CH₄ selectivity from 27.0 to 33.3 compared to the neat CTA/CDA blend membrane. The higher selectivity may have resulted from the enhanced molecular sieving capability provided by NH₂-ZIF-8

as its aperture size (3.4 Å) is between the kinetic diameters of CO₂ (3.3 Å) and CH₄ (3.8 Å) [26], while the larger permeability may have arisen from strong interaction among CO₂, imidazole linkers, and -NH₂ groups of NH₂-ZIF-8 that facilitated gas transport across the membrane [57]. However, a further increment in NH₂-ZIF-8 loading to 20 wt.% resulted in a lower CO₂/CH₄ selectivity of 24.4 but a higher CO₂ permeability of 13.2 Barrer. This is because a higher loading may generate nonselective voids. As a consequence, the CTA/CDA-15 wt.% NH₂-ZIF-8 blend MMM was selected for subsequent investigations.

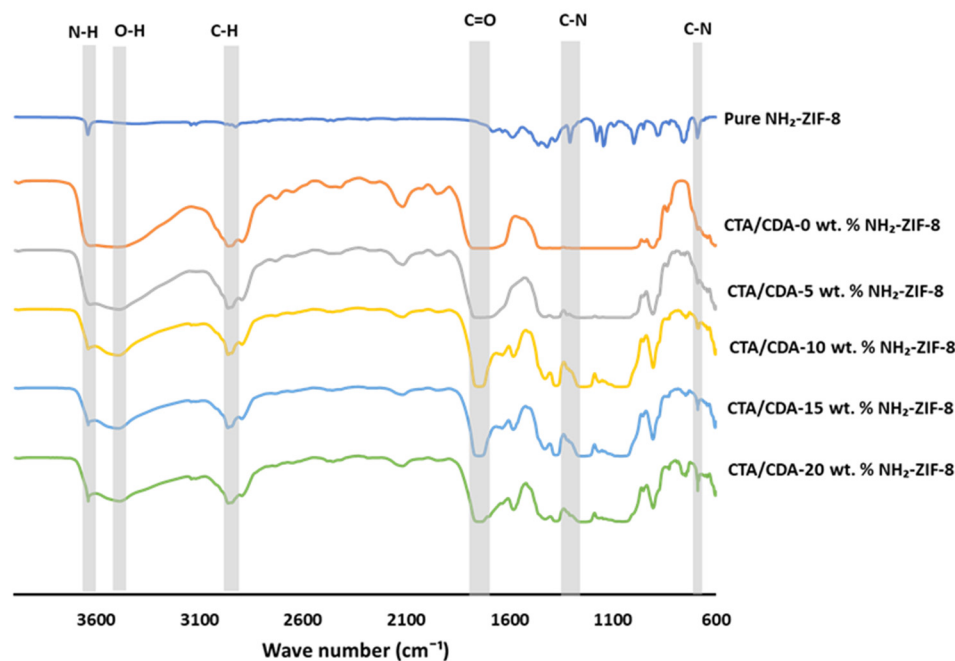


Figure 4. FTIR analyses of pure NH₂-ZIF-8 and CTA/CDA-NH₂-ZIF-8 MMMs with different NH₂-ZIF-8 loadings.

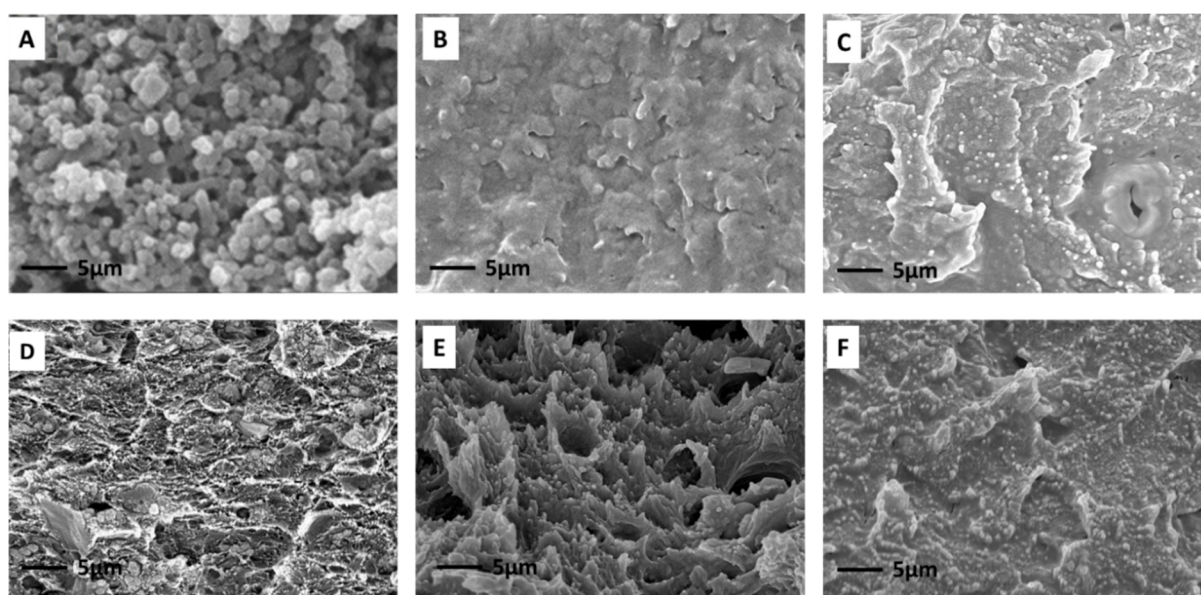


Figure 5. FESEM cross-section images of (A) pure NH₂-ZIF-8, (B) CTA/CDA-0 wt.% NH₂-ZIF-8, (C) CTA/CA-5 wt.% NH₂-ZIF-8, (D) CTA/CDA-10 wt.% NH₂-ZIF-8, (E) CTA/CDA-15 wt.% NH₂-ZIF-8, and (F) CTA/CDA-20 wt.% NH₂-ZIF-8.

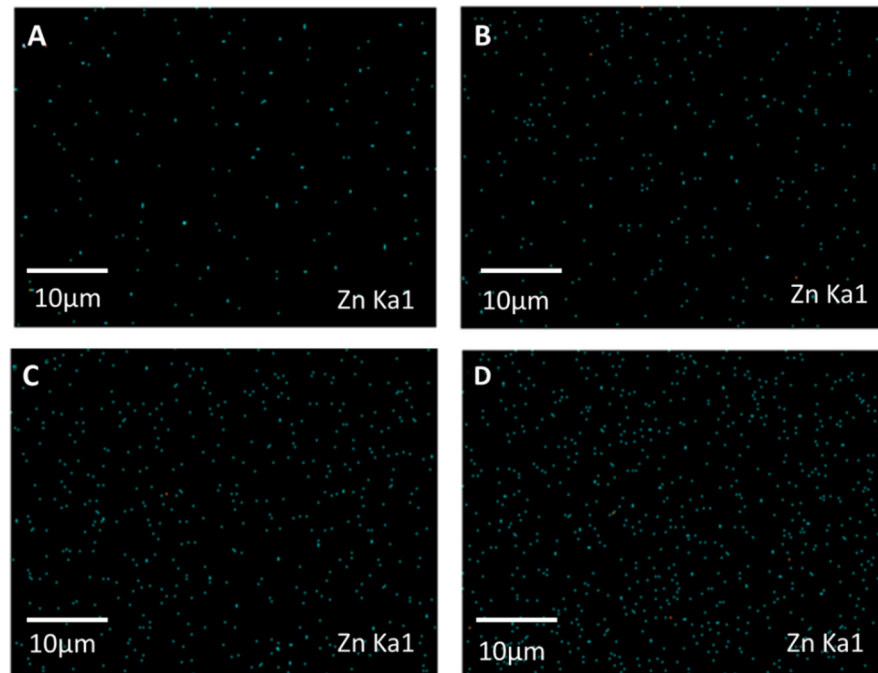


Figure 6. EDX analyses of (A) CTA/CDA-5 wt.% NH₂-ZIF-8, (B) CTA/CDA-10 wt.% NH₂-ZIF-8, (C) CTA/CDA-15 wt.% NH₂-ZIF-8, and (D) CTA/CDA-20 wt.% NH₂-ZIF-8.

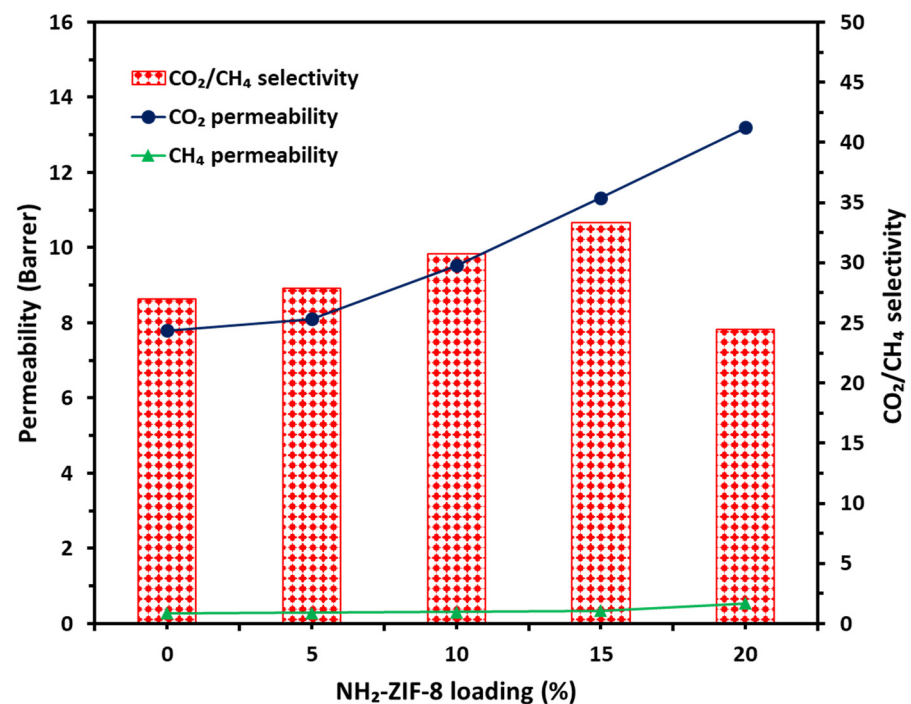


Figure 7. Separation performance of fabricated membranes as a function of NH₂-ZIF-8 loading.

3.2.1. Sorption Behavior of CO₂ and CH₄

Figure 8 presents the dual-mode Langmuir–Henry sorption behavior for both CO₂ and CH₄ in the pristine polymer blend and the optimized MMM. Both membranes showed higher CO₂ adsorption than CH₄ because of the inherently higher sorption affinity between the CTA/CDA polymer and CO₂ [58]. Table 2 summarizes their permeability, solubility, diffusivity coefficients, and selectivity. As expected, the CO₂ diffusivity and solubility coefficients showed 44% and 4% increases, respectively, when 15 wt.% NH₂-ZIF-8 was

incorporated into the CTA/CDA blend matrix. Consequently, the overall improvement in gas separation performance came from two factors; namely, the additional diffusive pathways and free volume provided by NH₂-ZIF-8. However, comparing the percentages of their increments, one can easily conclude that the former played a more important role than the latter to enhance the molecular sieving capability of the CTA/CDA blend membrane for CO₂/CH₄ separation, as observed in the literature [59].

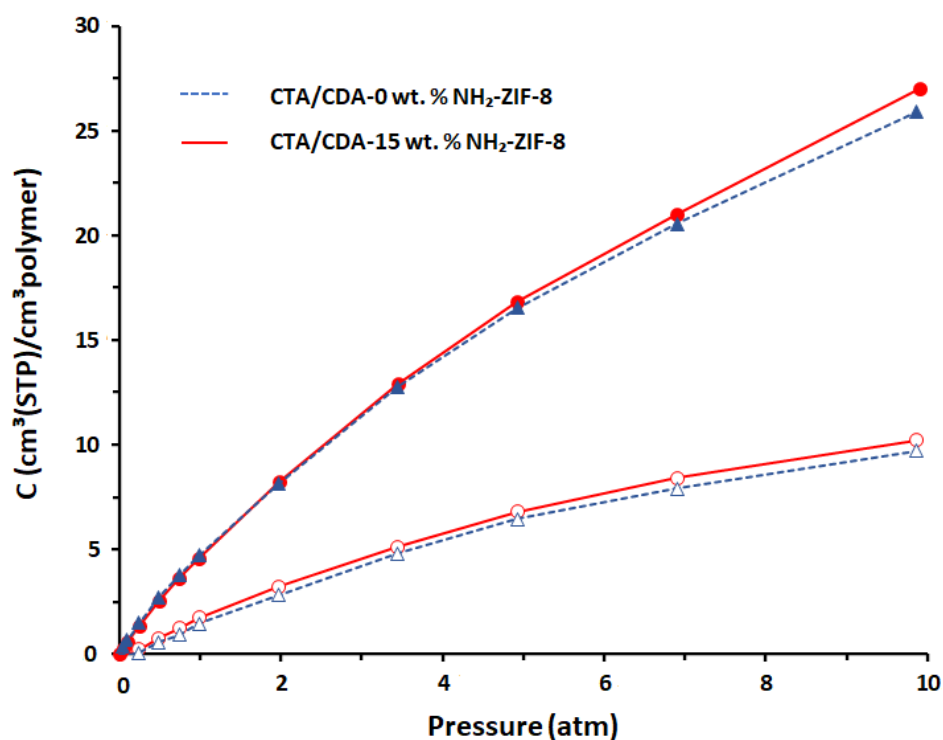


Figure 8. Sorption isotherms of CO₂ (closed symbols) and CH₄ (open symbols) in the pristine CTA/CDA-0 wt.% NH₂-ZIF-8 (solid blue line) and CTA/CDA-15 wt.% NH₂-ZIF-8 MMM (solid red line) as a function.

Table 2. Calculated pure gas permeabilities (Barrer), solubility coefficients (10^{-2} cm³ (STP)/cm³cm Hg), diffusivity coefficients (10^{-8} cm²/s), and corresponding selectivities of CO₂ and CH₄ for CTA/CDA-0 wt.% NH₂-ZIF-8 and CTA/CDA-15 wt.% NH₂-ZIF-8.

Sample Name	Pure CO ₂			Pure CH ₄			CO ₂ /CH ₄ Selectivity		
	P ^a	S ^b	D ^c	P ^a	S ^b	D ^c	α_P	α_S	α_D
CTA/CDA-0 wt.% NH ₂ -ZIF-8	7.56	3.47	2.18	0.28	1.29	0.22	27.00	2.69	10.04
CTA/CDA-15 wt.% NH ₂ -ZIF-8	11.33	3.61	3.14	0.34	1.35	0.25	33.33	2.67	12.46

^a Permeability (Barrer), ^b Solubility coefficients (10^{-2} cm³ (STP)/cm³cm Hg), ^c Diffusivity coefficients (10^{-8} cm²/s).

3.2.2. Plasticization Behavior and Mixed Gas Tests

To investigate the CO₂-induced plasticization phenomenon, the testing pressure of CO₂ was intermittently ramped from 5 to 25 bar at 35 °C. Figure 9 shows the CO₂-induced plasticization behavior of the pristine CTA/CDA blend membrane and the CTA/CDA-15 wt.% NH₂-ZIF-8 MMM. The former had a plasticization pressure of around 10.4 bar, while the latter showed a plasticization pressure of about 21.47 bar. The notable improvement in CO₂-induced plasticization pressure may have arisen from good compatibility and chain

interactions between the polymer matrix and NH₂-ZIF-8 molecules. The results are in good agreement with the literature [60].

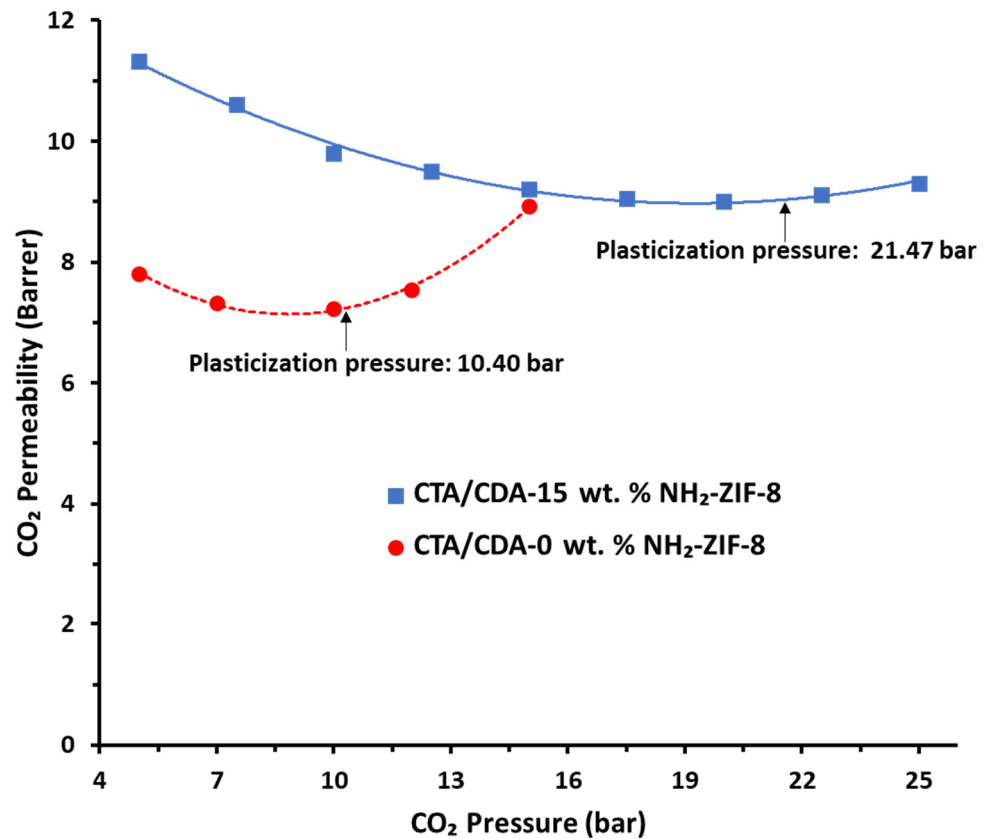


Figure 9. CO₂ plasticization behavior of the pristine CTA/CDA-0 wt.% NH₂-ZIF-8 blend membrane and CTA/CDA-15 wt.% NH₂-ZIF-8 blend MMM.

Table 3 compares the gas separation performance of the pristine CTA/CDA blend membrane and the optimized MMM under pure and mixed gas tests where a binary mixture of CO₂/CH₄ (50/50, *v/v*) was used as the mixed gas feed. Consistent with the literature, the mixed gas tests showed lower permeabilities for both CO₂ and CH₄ gases than the pure gas ones owing to the competitive diffusion and sorption between CO₂ and CH₄ molecules [61,62]. Since the percentage of permeability drop for CH₄ in the former was higher than that in the latter, this results in a higher CO₂/CH₄ selectivity in the mixed gas tests.

Table 3. Comparison of pure gas and mixed gas separation performance.

Sample Name	Pure Gas			Mixed Gas		
	CO ₂ (Barrer)	CH ₄ (Barrer)	Selectivity CO ₂ /CH ₄	CO ₂ (Barrer)	CH ₄ (Barrer)	Selectivity CO ₂ /CH ₄
CTA/CDA-0 wt.% NH ₂ -ZIF-8	7.56	0.28	27	6.70	0.22	30.22
CTA/CDA-15 wt.% NH ₂ -ZIF-8	11.33	0.34	33.32	9.50	0.23	41.09

3.3. Benchmark with the Literature

Table 4 benchmarks the pure-gas separation performance of the newly developed membranes with other CA membranes reported in the literature for CO₂ and CH₄ separation. The CTA/CDA-15 wt.% NH₂-ZIF-8 membrane showed higher separation perfor-

mance because its polymer matrix was made of a CTA/CDA blend that had inherently high gas separation performance and (2) it had 15 wt.% NH₂-ZIF-8 nanoparticles to enhance its gas diffusivity and molecular sieving characteristics.

Table 4. Comparison of pure-gas separation performance of cellulose acetate (CA)-based membranes in the literature.

Membrane Material	Pres. (Bar)	Temp. (°C)	CO ₂ (Barrer)	CH ₄ (Barrer)	CO ₂ /CH ₄	Ref.
CDA	11	35	3.9	0.11	35	[62]
CTA	4	35	6	0.3	20	[49]
CDA-CTA ^a	11	35	7.1	0.27	26	[34]
CA/nanoporous layered silicate AMH-3	4.6	-	10.36	0.35	30.03	[63]
CA/MWCNTs	2	Room temperature	14.21	0.66	21.20	[64]
P[CA][TF2N] ^b	1	25	8.9	0.4	22.25	[65]
CTA/[emim][BF ₄] ^c	4	35	12	0.6	20	[49]
CTA/CDA-0 wt.% NH ₂ -ZIF-8	5	35	7.56	0.28	27	This work
CTA/CDA-15 wt.% NH ₂ -ZIF-8	5	35	11.33	0.34	33.33	This work

^a 20-micron thickness. ^b poly(cellulose acetate)(bis(trifluoromethylsulfonyl)imide). ^c cellulose triacetate/1-ethyl-3-methylimidazolium tetrafluoroborate([emim][BF₄]).

4. Conclusions

We fabricated high-performance CTA/CDA-NH₂-ZIF-8 MMMs for CO₂/CH₄ separation. A solvo-chemical method was employed to synthesize NH₂-ZIF-8 nanocrystals with a particle size of 50–80 nm. Gas separation performance of the fabricated membranes have been investigated as a function of NH₂-ZIF-8 loading. The following conclusions can be drawn:

1. There is a linear relationship between permeability and NH₂-ZIF-8 loading. However, the relationship changes to a π -shape between CO₂/CH₄ selectivity and NH₂-ZIF-8 loading due to void formation. Thus, there is an optimum loading to fabricate CTA/CDA based MMMs with high gas separation performance.
2. The optimized MMM contained 15 wt.% of NH₂-ZIF-8 nanoparticles and had a CO₂ permeability of 11.33 Barrer which was 50% higher than the pristine CTA/CDA membrane. In addition, the former had a superior CO₂/CH₄ selectivity of 33.33 to the latter of 27 under pure gas tests.
3. The enhanced molecular sieving capability and additional free volume provided by NH₂-ZIF-8 nanoparticles improved the CO₂ diffusivity and solubility coefficients by 44% and 4%, respectively, under pure gas tests when 15 wt.% NH₂-ZIF-8 was incorporated into the CTA/CDA membrane.
4. The CO₂/CH₄ selectivity can be further increased to 41 under mixed gas tests due to the competitive diffusion and sorption between CO₂ and CH₄ molecules.
5. A notable improvement in CO₂-induced plasticization pressure from 10.4 to 21.47 bar was observed owing to the good compatibility and chain interactions between CTA/CDA and NH₂-ZIF-8 molecules.

Therefore, the newly fabricated polymer blend MMMs may have great potential for CO₂ separation in the natural gas industry.

Author Contributions: Conceptualization, A.R. and S.F.; methodology, A.R. and S.J.; investigation, A.R., S.J. and C.Z.L.; resources, A.H. and T.-S.C.; writing—original draft preparation, A.R.; writing—review and editing, A.R., S.F., S.J., C.Z.L. and T.-S.C.; supervision, A.H. and T.-S.C. All authors have read and agreed to the published version of the manuscript.

Funding: The authors would like to thank the Singapore Energy Centre (SgEC) under the project entitled “Design of novel mixed matrix membranes and thin-film composite membranes for ultra-

efficient hydrogen separation and CO₂ capture” (Grant number: R-261–517-004-592) for funding this re-search.

Institutional Review Board Statement: Not applicable.

Informed Consent Statement: Not applicable.

Data Availability Statement: The data presented in this study are available on request from the corresponding author.

Acknowledgments: Thanks are also due to the Higher Education Commission, Pakistan and Membranes for applied research (MEMAR) laboratory, School of Chemical and Materials Engineering (SCME), National University of Sciences and Technology (NUST), Pakistan for the award of International Research Support Initiative Program (IRSIP). Professor Chung would also like to thank the Yushan Scholar Program supported by the Ministry of Education, Taiwan.

Conflicts of Interest: The authors declare no conflict of interest.

References

1. Baker, R.W.; Lokhandwala, K. Natural gas processing with membranes: An overview. *Ind. Eng. Chem. Res.* **2008**, *47*, 2109–2121. [[CrossRef](#)]
2. Shah, M.S.; Tsapatsis, M.; Siepmann, J.I. Hydrogen sulfide capture: From absorption in polar liquids to oxide, zeolite, and metal–organic framework adsorbents and membranes. *Chem. Rev.* **2017**, *117*, 9755–9803. [[CrossRef](#)]
3. Mazyan, W.; Ahmadi, A.; Ahmed, H.; Hoorfar, M. Market and technology assessment of natural gas processing: A review. *J. Nat. Gas Sci. Eng.* **2016**, *30*, 487–514. [[CrossRef](#)]
4. Bhide, B.; Stern, S. Membrane processes for the removal of acid gases from natural gas. II. Effects of operating conditions, economic parameters, and membrane properties. *J. Membr. Sci.* **1993**, *81*, 239–252. [[CrossRef](#)]
5. Baker, R.W. *Membrane Technology and Applications*, 3rd ed.; John Wiley & Sons: Newark, CA, USA, 2012; pp. 325–373.
6. Bernardo, P.; Drioli, E.; Golemme, G. Membrane gas separation: A review/state of the art. *Ind. Eng. Chem. Res.* **2009**, *48*, 4638–4663. [[CrossRef](#)]
7. Xiao, Y.; Low, B.T.; Hosseini, S.S.; Chung, T.S.; Paul, D.R. The strategies of molecular architecture and modification of polyimide-based membranes for CO₂ removal from natural gas—A review. *Prog. Polym. Sci.* **2009**, *34*, 61–580. [[CrossRef](#)]
8. Koros, W.; Fleming, G.; Jordan, S.; Kim, T.; Hoehn, H. Polymeric membrane materials for solution-diffusion based permeation separations. *Prog. Polym. Sci.* **1988**, *13*, 339–401. [[CrossRef](#)]
9. Dong, G.; Li, H.; Chen, V. Challenges and opportunities for mixed-matrix membranes for gas separation. *J. Mater. Chem. A* **2013**, *1*, 4610–4630. [[CrossRef](#)]
10. Liang, C.Z.; Chung, T.S.; Lai, J.-Y. A review of polymeric composite membranes for gas separation and energy production. *Prog. Polym. Sci.* **2019**, *97*, 101141. [[CrossRef](#)]
11. Han, Y.; Zhang, Z. Nanostructured membrane materials for CO₂ capture: A critical review. *J. Nano Sci.* **2019**, *19*, 3173–3179. [[CrossRef](#)]
12. Shah, S.; Shah, M.; Shah, A.; Shah, M. Evolution in the membrane-based materials and comprehensive review on carbon capture and storage in industries. *Emerg. Mater.* **2020**, *3*, 33–44. [[CrossRef](#)]
13. Lin, H.; Yavari, M. Upper bound of polymeric membranes for mixed-gas CO₂/CH₄ separations. *J. Membr. Sci.* **2015**, *475*, 101–109. [[CrossRef](#)]
14. Robeson, L.M. The upper bound revisited. *J. Membr. Sci.* **2008**, *320*, 390–400. [[CrossRef](#)]
15. Suleman, M.S.; Lau, K.K.; Yeong, Y.F. Plasticization and swelling in polymeric membranes in CO₂ removal from natural gas. *Chem. Eng. Technol.* **2016**, *39*, 1604–1616. [[CrossRef](#)]
16. Minelli, M.; Oradei, S.; Fiorini, M.; Sarti, G.C. CO₂ plasticization effect on glassy polymeric membranes. *Polymer* **2019**, *163*, 29–35. [[CrossRef](#)]
17. Ismail, A.F.; Lorna, W. Penetrant-induced plasticization phenomenon in glassy polymers for gas separation membrane. *Sep. Purif. Technol.* **2002**, *27*, 173–194. [[CrossRef](#)]
18. Kim, S.; Lee, Y.M. High performance polymer membranes for CO₂ separation. *Curr. Opin. Chem. Eng.* **2013**, *2*, 238–244. [[CrossRef](#)]
19. Yong, W.F.; Zhang, H. Recent advances in polymer blend membranes for gas separation and pervaporation. *Prog. Mater. Sci.* **2020**, *116*, 100713. [[CrossRef](#)]
20. Vinoba, M.; Bhagiyalakshmi, M.; Alqaheem, Y.; Alomair, A.A.; Pérez, A.; Rana, M.S. Recent progress of fillers in mixed matrix membranes for CO₂ separation: A review. *Sep. Purif. Technol.* **2017**, *188*, 431–450. [[CrossRef](#)]
21. Guan, W.; Dai, Y.; Dong, C.; Yang, X.; Xi, Y. Zeolite imidazolate framework (ZIF)-based mixed matrix membranes for CO₂ separation: A review. *J. Appl. Polym. Sci.* **2020**, *137*, 48968. [[CrossRef](#)]
22. Wang, B.; Sheng, M.; Xu, J.; Zhao, S.; Wang, J.; Wang, Z. Recent advances of gas transport channels constructed with different dimensional nanomaterials in mixed-matrix membranes for CO₂ separation. *Small Methods* **2020**, *4*, 1900749. [[CrossRef](#)]

23. Askari, M.; Chung, T.S. Natural gas purification and olefin/paraffin separation using thermal cross-linkable co-polyimide/ZIF-8 mixed matrix membranes. *J. Membr. Sci.* **2013**, *444*, 173–183. [[CrossRef](#)]
24. Lai, Z. Development of ZIF-8 membranes: Opportunities and challenges for commercial applications. *Curr. Opin. Chem. Eng.* **2018**, *20*, 78–85. [[CrossRef](#)]
25. Gong, X.; Wang, Y.; Kuang, T. ZIF-8-based membranes for carbon dioxide capture and separation. *ACS Sustain. Chem. Eng.* **2017**, *5*, 11204–11214. [[CrossRef](#)]
26. Hopfenberg, H.; Paul, D.R. Transport phenomena in polymer blends. In *Polymer Blends*, 1st ed.; Elsevier: Amsterdam, The Netherlands, 1978; Volume 1, pp. 445–489. [[CrossRef](#)]
27. Mahajan, R.; Burns, R.; Schaeffer, M.; Koros, W.J. Challenges in forming successful mixed matrix membranes with rigid polymeric materials. *J. Appl. Polym. Sci.* **2002**, *86*, 881–890. [[CrossRef](#)]
28. Chung, T.S.; Jiang, L.Y.; Li, Y.; Kulprathipanja, S. Mixed matrix membranes (MMMs) comprising organic polymers with dispersed inorganic fillers for gas separation. *Prog. Polym. Sci.* **2007**, *32*, 483–507. [[CrossRef](#)]
29. Li, J.; Nagai, K.; Nakagawa, T.; Wang, S. Preparation of polyethyleneglycol (PEG) and cellulose acetate (CA) blend membranes and their gas permeabilities. *J. Appl. Polym. Sci.* **1995**, *58*, 1455–1463. [[CrossRef](#)]
30. Li, J.; Wang, S.; Nagai, K.; Nakagawa, T.; Mau, A.W. Effect of polyethyleneglycol (PEG) on gas permeabilities and permselectivities in its cellulose acetate (CA) blend membranes. *J. Membr. Sci.* **1998**, *138*, 143–152. [[CrossRef](#)]
31. Sajjan, P.; Nayak, V.; Padaki, M.; Zadorozhnyy, V.Y.; Klyamkin, S.N.; Konik, P. Fabrication of cellulose acetate film through blending technique with palladium acetate for hydrogen gas separation. *Energy Fuel* **2020**, *34*, 11699–11707. [[CrossRef](#)]
32. Sanaeepur, H.; Ahmadi, R.; Sinaei, M.; Kargari, A. Pebax-modified cellulose acetate membrane for CO₂/N₂ separation. *J. Membr. Sci.* **2019**, *5*, 25–32.
33. Akbarzadeh, E.; Shockravi, A.; Vatanpour, V. High performance compatible thiazole-based polymeric blend cellulose acetate membrane as selective CO₂ absorbent and molecular sieve. *Carbohydr. Polym.* **2021**, *252*, 117215. [[CrossRef](#)] [[PubMed](#)]
34. Nguyen, H.; Hsiao, M.-Y.; Nagai, K.; Lin, H. Suppressed crystallization and enhanced gas permeability in thin films of cellulose acetate blends. *Polymer* **2020**, *205*, 122790. [[CrossRef](#)]
35. Pan, Y.; Liu, Y.; Zeng, G.; Zhao, L.; Lai, Z. Rapid synthesis of zeolitic imidazolate framework-8 (ZIF-8) nanocrystals in an aqueous system. *Chem. Commun.* **2011**, *47*, 2071–2073. [[CrossRef](#)] [[PubMed](#)]
36. Nordin, N.A.H.M.; Racha, S.M.; Matsuura, T.; Misdan, N.; Sani, N.A.A.; Ismail, A.F.; Mustafa, A. Facile modification of ZIF-8 mixed matrix membrane for CO₂/CH₄ separation: Synthesis and preparation. *RSC Adv.* **2015**, *5*, 43110–43120. [[CrossRef](#)]
37. Liu, D.; Wu, Y.; Xia, Q.; Li, Z.; Xi, H. Experimental and molecular simulation studies of CO₂ adsorption on zeolitic imidazolate frameworks: ZIF-8 and amine-modified ZIF-8. *Adsorption* **2013**, *19*, 25–37. [[CrossRef](#)]
38. Chen, H.Z.; Xiao, Y.C.; Chung, T.S. Synthesis and characterization of poly (ethylene oxide) containing copolyimides for hydrogen purification. *Polymer* **2010**, *51*, 4077–4086. [[CrossRef](#)]
39. Yong, W.F.; Chung, T.S. Mechanically strong and flexible hydrolyzed polymers of intrinsic microporosity (PIM1) membranes. *J. Polym. Sci. Part B Polym. Phys.* **2017**, *55*, 344–354. [[CrossRef](#)]
40. Wang, R.; Liu, S.; Lin, T.; Chung, T.S. Characterization of hollow fiber membranes in a permeator using binary gas mixtures. *Chem. Eng. Sci.* **2002**, *57*, 967–976. [[CrossRef](#)]
41. Park, K.S.; Ni, Z.; Côté, A.P.; Choi, J.Y.; Huang, R.; Uribe-Romo, F.J.; Chae, H.K.; O’Keeffe, M.; Yaghi, O.M. Exceptional chemical and thermal stability of zeolitic imidazolate frameworks. *Proc. Natl. Acad. Sci. USA* **2006**, *103*, 10186–10191. [[CrossRef](#)]
42. Song, Q.; Nataraj, S.; Roussenova, M.V.; Tan, J.C.; Hughes, D.J.; Li, W.; Bourgoïn, P.; Alam, M.A.; Cheetham, A.K.; Al-Muhtaseb, S.A. Zeolitic imidazolate framework (ZIF-8) based polymer nanocomposite membranes for gas separation. *Energy Environ. Sci.* **2012**, *5*, 8359–8369. [[CrossRef](#)]
43. Chatterjee, P.K.; Conrad, C.M. Thermogravimetric analysis of cellulose. *J. Polym. Sci. Part A1 Polym. Chem.* **1968**, *6*, 3217–3233. [[CrossRef](#)]
44. Kamal, H.; Abd-Elrahim, F.; Lotfy, S. Characterization and some properties of cellulose acetate-co-polyethylene oxide blends prepared by the use of gamma irradiation. *J. Radiat. Res. Appl. Sci.* **2014**, *7*, 146–153. [[CrossRef](#)]
45. Arthanareeswaran, G.; Thanikaivelan, P.; Srinivasn, K.; Mohan, D.; Rajendran, M. Synthesis, characterization and thermal studies on cellulose acetate membranes with additive. *Eur. Polym. J.* **2004**, *40*, 2153–2159. [[CrossRef](#)]
46. Abedini, R.; Mousavi, S.M.; Aminzadeh, R. A novel cellulose acetate (CA) membrane using TiO₂ nanoparticles: Preparation, characterization and permeation study. *Desalination* **2011**, *277*, 40–45. [[CrossRef](#)]
47. Jamil, A.; Zulfiqar, M.; Arshad, U.; Mahmood, S.; Iqbal, T.; Rafiq, S.; Iqbal, M.Z. Development and performance evaluation of cellulose acetate-bentonite mixed matrix membranes for CO₂ separation. *Adv. Polym. Technol.* **2020**, *2020*. [[CrossRef](#)]
48. Kamide, K.; Saito, M. Thermal analysis of cellulose acetate solids with total degrees of substitution of 0.49, 1.75, 2.46, and 2.92. *Polym. J.* **1985**, *17*, 919–928. [[CrossRef](#)]
49. Lam, B.; Wei, M.; Zhu, L.; Luo, S.; Guo, R.; Morisato, A.; Alexandridis, P.; Lin, H. Cellulose triacetate doped with ionic liquids for membrane gas separation. *Polymer* **2016**, *89*, 1–11. [[CrossRef](#)]
50. Nordin, N.A.H.M.; Ismail, A.F.; Misdan, N.; Nazri, N.A.M. Modified ZIF-8 mixed matrix membrane for CO₂/CH₄ separation. In *AIP Conference Proceedings*; AIP Publishing LLC: Melville, NY, USA, 2017.
51. Isanejad, M.; Arzani, M.; Mahdavi, H.R.; Mohammadi, T. Novel amine modification of ZIF-8 for improving simultaneous removal of cationic dyes from aqueous solutions using supported liquid membrane. *J. Mol. Liq.* **2017**, *225*, 800–809. [[CrossRef](#)]

52. Pavia, D.L.; Lampman, G.M.; Kriz, G.S.; Vyvyan, J.A. *Introduction to Spectroscopy*, 5th ed.; Nelson Education: Stanford, CA, USA, 2014; pp. 14–86.
53. Yuan, J.; Li, Q.; Shen, J.; Huang, K.; Liu, G.; Zhao, J.; Duan, J.; Jin, W. Hydrophobic functionalized ZIF8 nanoparticles incorporated PDMS membranes for high selective separation of propane/nitrogen. *Asia-Pac. J. Chem. Eng.* **2017**, *12*, 110–120. [[CrossRef](#)]
54. Wang, S.; Cui, J.; Zhang, S.; Xie, X.; Xia, W. Enhancement thermal stability and CO₂ adsorption property of ZIF-8 by pre-modification with polyaniline. *Mater. Res. Express* **2020**, *7*, 025304. [[CrossRef](#)]
55. Jusoh, N.; Yeong, Y.F.; Lau, K.K.; Shariff, A.M. Mixed matrix membranes comprising of ZIF-8 nanofillers for enhanced gas transport properties. *Procedia Eng.* **2016**, *148*, 1259–1265. [[CrossRef](#)]
56. Yeong, Y.F.; Wang, H.; Pramoda, K.P.; Chung, T.S. Thermal induced structural rearrangement of cardo-copolybenzoxazole membranes for enhanced gas transport properties. *J. Membr. Sci.* **2012**, *397*, 51–65. [[CrossRef](#)]
57. Heering, C.; Boldog, I.; Vasylyeva, V.; Sanchiz, J.; Janiak, C. Bifunctional pyrazolate–carboxylate ligands for isoreticular cobalt and zinc MOF-5 analogs with magnetic analysis of the {Co₄(μ₄-O)} node. *CrystEngComm* **2013**, *15*, 9757–9768. [[CrossRef](#)]
58. Sada, E.; Kumazawa, H.; Xu, P.; Wang, S.T. Permeation of pure carbon dioxide and methane and binary mixtures through cellulose acetate membranes. *J. Polym. Sci.* **1990**, *28*, 113–125. [[CrossRef](#)]
59. Zhang, L.; Wu, G.; Jiang, J. Adsorption and diffusion of CO₂ and CH₄ in zeolitic imidazolate framework-8: Effect of structural flexibility. *J. Phys. Chem. C* **2014**, *118*, 8788–8794. [[CrossRef](#)]
60. Japip, S.; Wang, H.; Xiao, Y.; Chung, T.S. Highly permeable zeolitic imidazolate framework (ZIF)-71 nano-particles enhanced polyimide membranes for gas separation. *J. Membr. Sci.* **2014**, *467*, 162–174. [[CrossRef](#)]
61. Zhang, C.; Dai, Y.; Johnson, J.R.; Karvan, O.; Koros, W.J. High performance ZIF-8/6FDA-DAM mixed matrix membrane for propylene/propane separations. *J. Membr. Sci.* **2012**, *389*, 34–42. [[CrossRef](#)]
62. Nguyen, H.; Wang, M.; Hsiao, M.-Y.; Nagai, K.; Ding, Y.; Lin, H. Suppression of crystallization in thin films of cellulose diacetate and its effect on CO₂/CH₄ separation properties. *J. Membr. Sci.* **2019**, *586*, 7–14. [[CrossRef](#)]
63. Kim, W.G.; Lee, J.S.; Bucknall, D.G.; Koros, W.J.; Nair, S. Nanoporous layered silicate AMH-3/cellulose acetate nanocomposite membranes for gas separations. *J. Membr. Sci.* **2013**, *441*, 129–136. [[CrossRef](#)]
64. Moghadassi, A.; Rajabi, Z.; Hosseini, S.; Mohammadi, M. Fabrication and modification of cellulose acetate based mixed matrix membrane: Gas separation and physical properties. *J. Ind. Eng. Chem.* **2014**, *20*, 1050–1060. [[CrossRef](#)]
65. Nikolaeva, D.; Azcune, I.; Tanczyk, M.; Warmuzinski, K.; Jaschik, M.; Sandru, M.; Dahl, P.I.; Genua, A.; Lois, S.; Sheridan, E. The performance of affordable and stable cellulose-based poly-ionic membranes in CO₂/N₂ and CO₂/CH₄ gas separation. *J. Membr. Sci.* **2018**, *564*, 552–561. [[CrossRef](#)]